Cell, Vol. 111, 981–990, December 27, 2002, Copyright ©2002 by Cell Press

# PKCγ Regulates Syndecan-2 Inside-Out Signaling during *Xenopus* Left-Right Development

**Kenneth L. Kramer, Janet E. Barnette, and H. Joseph Yost**[1]
Center for Children, Huntsman Cancer Institute
Department of Oncological Sciences and
Department of Pediatrics
University of Utah
2000 Circle of Hope
Salt Lake City, Utah 84112

## Summary

**The transmembrane proteoglycan syndecan-2 cell nonautonomously regulates left-right (LR) development in migrating mesoderm by an unknown mechanism, leading to LR asymmetric gene expression and LR orientation of the heart and gut. Here, we demonstrate that protein kinase C γ (PKCγ) mediates phosphorylation of the cytoplasmic domain of syndecan-2 in right, but not left, animal cap ectodermal cells. Notably, both phosphorylation states of syndecan-2 are obligatory for normal LR development, with PKCγ-dependent phosphorylated syndecan-2 in right ectodermal cells and nonphosphorylated syndecan-2 in left cells. The ectodermal cells contact migrating mesodermal cells during early gastrulation, concurrent with the transmission of LR information. This precedes the appearance of monocilia and is one of the earliest steps of LR development. These results demonstrate that PKCγ regulates the cytoplasmic phosphorylation of syndecan-2 and, consequently, syndecan-2-mediated inside-out signaling to adjacent cells.**

## Introduction

Formation of the three germ layers during vertebrate gastrulation converts the radially symmetric blastoderm into a bilaterally symmetric embryo with morphologically distinct anterior-posterior and dorsal-ventral axes. Shortly thereafter, asymmetric expression of *nodal*, *lefty2*, and *pitx2* in the left lateral plate mesoderm have been observed throughout vertebrates even though LR asymmetries in the shape and position of internal organs do not arise until much later in development (reviewed in Hamada et al., 2002). How and when the lateral plate mesoderm is patterned with LR axial information has been a subject of considerable debate (Capdevila et al., 2000; Hamada et al., 2002; Wright, 2001).

Microtubule motor molecules in the mouse embryonic node appear to participate in the generation of a directional asymmetric extracellular flow during early somitogenesis (Nonaka et al., 2002, 1998; Okada et al., 1999). This asymmetric nodal flow has also been implicated in patterning lateral plate mesoderm (Nonaka et al., 2002). Monocilia and expression of a dynein molecule have been observed in a small group of cells in mice, chick, frog, and zebrafish gastrula, suggesting that they have a conserved role in vertebrates and by inference, that nodal flow is conserved throughout vertebrates (Essner et al., 2002). However, it is not clear whether nodal flow is the first step in LR development in vertebrates or a necessary intermediate step. Furthermore, functional roles of monocilia have not been demonstrated in vertebrates other than mouse.

In *Xenopus*, several experiments suggest that the LR axis is initiated before monocilia even appear in cells derived from Spemann's Organizer. Manipulations of microtubules during the first cell cycle (Danos and Yost, 1995; Yost, 1991) and gap junctions from blastula through late gastrula stages (Levin and Mercola, 1998) disrupt normal LR development. Recent pharmacological inhibitor studies indicate that H+/K+-ATPase activity is required for normal LR development from the first cell cycle to approximately the midblastula transition (Levin et al., 2002). These observations suggest that the pathways that establish LR asymmetry occur prior to the appearance of monocilia at the end of gastrulation.

We recently established that the cell surface heparan sulfate proteoglycan syndecan-2 functions in the ectoderm by transmitting LR information to migrating mesoderm (Kramer and Yost, 2002). Mesodermal cell migration occurs during gastrulation, so the syndecan-2-dependent transmission of LR information could be concurrent with or prior to nodal flow. However, in order to block subsequent LR development (including normal *nodal*, *lefty*, and *pitx2* asymmetric expression and organ orientation), a dominant-negative syndecan-2 must be functional during early gastrulation (Kramer and Yost, 2002), well before LR-dynein gene expression and before monocilia appear in *Xenopus* (Essner et al., 2002). This suggests that LR developmental pathways are initiated in the ectoderm before the formation of monocilia and include syndecan-2 as a component.

Early LR developmental components need not function asymmetrically. Syndecan-2 and other factors could function asymmetrically, as a LR instructive molecule, or symmetrically, as a bilaterally permissive molecule. In a well-known example, the EGF-CFC genes are involved in LR development in several vertebrates but do not appear to function as asymmetrically instructive molecules per se (Bamford et al., 2000; Gaio et al., 1999; Shen and Schier, 2000; Yan et al., 1999). EGF-CFCs are cofactors that are necessary for signaling by the TGFβ ligand nodal (Gritsman et al., 1999), but their role in LR development appears to be permissive, not instructive. EGF-CFC needs to be present, but it is nodal signaling that instructs normal LR development in lateral plate mesoderm (Bamford et al., 2000; Gaio et al., 1999; Yan et al., 1999). Analogously, it is possible that syndecan-2 is merely a permissive factor in ectoderm to mesoderm cell signaling.

Here, we demonstrate that syndecan-2 has an asymmetric, instructive function in *Xenopus* LR development, which is mediated by the phosphorylation of the cytoplasmic domain of syndecan-2 in right, but not left, ectoderm. Furthermore, syndecan-2 phosphorylation is dependent on the upstream activity of PKCγ. The re-

[1]Correspondence: joseph.yost@hci.utah.edu

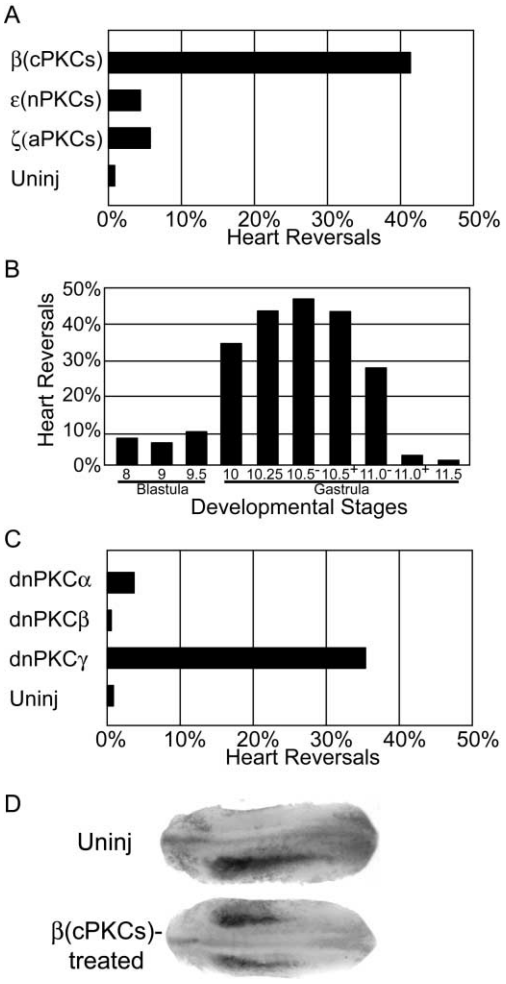


Figure 1. PKCγ Regulates LR Development during Early Gastrulation

(A) Percentage of reversed heart looping in embryos injected with cell-permeable PKC inhibitors into the blastocoel of stage 10.5 embryos. Myristoylated peptides (β, ϵ, ζ) block translocation and function of conventional (cPKCs), novel (nPKCs), or atypical (aPKCs) PKCs, respectively. (B) Percentage of reversed heart looping in embryos injected with the β myristoylated peptide that blocks cPKCs. The blastocoel was injected at several stages ranging from blastula to late gastrula. (C) Percentage of reversed heart looping in embryos injected with mRNA encoding dominant-negative (dn) PKC constructs for each of the cPKCs (α, β, or γ). n > 100 for each injection. (D) Representative in situ hybridizations of *Xnr1* in the lateral plate mesoderm illustrating the most prevalent expression classes: uninjected embryos display *Xnr1* expression on the left, and β myristoylated peptide-injected embryos display bilateral *Xnr1* expression. Panels are dorsal views with anterior to the left.

quirement for PKCγ activity and the concomitant phosphorylation of endogenous syndecan-2 occur prior to the onset of LR-dynein gene expression and monocilia formation. PKCγ-mediated phosphorylation of syndecan-2 in the ectoderm participates in establishing the LR axis in *Xenopus* during gastrulation, indicating that syndecan-2 can function as an inside-out transducer of LR patterning information.

## Results

### Normal LR Development Requires PKCγ Function in Early Gastrula

Because PKC family members have been shown to phosphorylate syndecan family members in vitro (Oh et al., 1997; Prasthofer et al., 1995) and in cell culture (Horowitz and Simons, 1998; Itano et al., 1996), we hypothesized that a PKC might regulate early LR development in embryos. To rapidly identify if any vertebrate PKCs are involved in LR development, our first approach was to incubate *Xenopus* embryos with the PKC pharmacological inhibitor chelerythrine chloride. When embryos were incubated in chelerythrine chloride from just after fertilization through early neurulation (stage 15), 19% of the embryos had hearts that were oriented in the opposite direction at 5 days in development (n = 59). This result suggested that PKCs might be involved in early LR development before the asymmetric expression of *nodal*, *lefty*, and *pitx2* in lateral plate mesoderm at tailbud stages (Hyatt et al., 1996; Meno et al., 1997; Ryan et al., 1998). Thus, we utilized more specific cell-permeable peptide inhibitors that selectively block the function of subgroups of PKCs (Ron et al., 1995). In vertebrates, there are at least 11 isoforms of PKC that can be clustered into conventional (cPKC), novel, and atypical subgroups. A peptide inhibitor of the cPKCs specifically randomized heart (Figure 1A) and gut looping (data not shown) with no other obvious morphological defects, whereas inhibitors of other PKC subclasses had no effects on LR development.

In order to assess the specific stages during which cPKCs are required for LR development, the cell-permeable cPKC inhibitor was injected into the blastocoel at specific stages of early development. For normal LR development, cPKCs are specifically required during early gastrula stages (Figure 1B), but not in earlier or later stages of development. It is noteworthy that the early gastrula stage during which a cPKC is required for LR development is significantly earlier than the expression of dynein or monocilia in the *Xenopus* organizer at the end of gastrulation.

To determine which cPKC is involved in LR, we utilized dominant-negative (dn) mutants of each member of the cPKC subgroup. The mutations were in the kinase domain of PKC, resulting in kinase-dead dnPKCs (Freisewinkel et al., 1991). mRNAs encoding each dnPKC were individually targeted to the animal cap ectoderm by injecting both ventral animal-pole cells in the 32-cell embryo. Only the dnPKCγ disrupted normal LR development (Figure 1C). The dnPKCγ effect on LR development was titrated by coinjection of wild-type PKCγ mRNA (data not shown). Together, the results with peptide inhibitors and dominant-negative inhibitors indicate that PKCγ in embryonic ectoderm specifically mediates LR development during early gastrulation.

Expression of the TGFβ signaling molecule *nodal* in the left lateral plate mesoderm is conserved among vertebrates and is downstream of syndecan-2 function in *Xenopus* (Kramer and Yost, 2002). To confirm that *nodal* is also downstream of PKC, we examined the expression of the relevant *Xenopus* homolog of nodal, *Xnr1*, by in situ hybridization in embryos injected with the cPKC

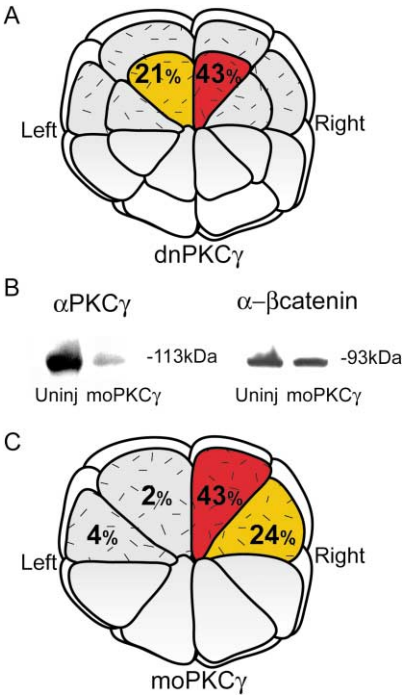


Figure 2. PKCγ Asymmetrically Regulates LR Development and Is Required in Right-Side Ectoderm

(A) Percentage of reversed heart looping in embryos injected with mRNA encoding dnPKCγ. The schematic animal-pole view of a 32-cell embryo illustrates the percentage of reversed heart looping observed when the corresponding cell was injected. Red indicates high reversal rates, yellow is intermediate reversal rates, and gray is background rates. Top is ventral. $n > 69$ for each injection. (B) Western blots of homogenates from stage 11 uninjected and morpholino (mo)-treated embryos probed with antibodies to PKCγ and β-catenin. (C) Percentage of reversed heart looping in embryos injected with anti-PKCγ morpholinos. Schematic is the same as in (A), except a 16-cell embryo is illustrated. $n > 60$ for each injection.

peptide inhibitor at stage 10.5 (Figure 1D). In treated embryos, *Xnr1* expression was predominantly bilateral (48%, $n = 46$; 20% left sided, 17% absent, 15% right sided), indicating that PKC functions upstream of the earliest known asymmetric gene transcription in *Xenopus*.

### PKCγ Functions Asymmetrically in LR Development

Two complementary approaches were used to begin to assess whether PKCγ is a permissive or instructive signal in early LR development. First, specific left or right ectodermal lineages were targeted with dnPKCγ. Heart looping was preferentially randomized when dnPKCγ was targeted to the right ectoderm (Figure 2A). Second, endogenous PKCγ synthesis was inhibited by antisense morpholinos in specific left or right ectodermal lineages. We cloned and characterized *Xenopus* PKCγ transcripts (see Supplemental Figure S1 online at http://www.cell.com/cgi/content/full/111/7/981/DC1) and designed antisense morpholino oligonucleotides that are complementary to the 5′UTRs. Injection of antisense morpholinos at the 2-cell stage reduced endogenous xPKCγ protein levels to 15% of uninjected controls when assayed at stage 11 and normalized to β-catenin (Figure 2B). Morpholinos targeted to right ectodermal cell lineages disrupted the orientation of heart looping (Figure 2C). In contrast, no effect on LR development was observed when morpholinos were targeted to left ectodermal cell lineages (Figure 2C).

To confirm that PKCγ mediates LR development in the ectoderm where it is endogenously expressed (Otte et al., 1991), we targeted the PKCγ morpholinos to the lateral plate mesoderm and endoderm by injecting the ventral vegetal cell lineages at the 8-cell stage and observed no effect on LR development (3% reversed hearts, $n = 78$). The lack of morpholino effect on the left side indicated that the effect on the right side was unlikely to be a nonspecific effect of morpholino injection. The lack of morpholino effect when injected into mesoderm precursors indicates that the function of xPKCγ in left-right development is restricted to ectodermal lineages. As an additional control, we asked whether the PKCγ morpholino effect could be abrogated by reintroduction of exogenous PKCγ. Normal heart looping was significantly rescued when a full-length mouse PKCγ (with distinct a 5′UTR that does not match the *Xenopus* morpholino sequence) was coinjected with the morpholinos into the right ectoderm (16% heart reversals, $n = 73$, $p < 0.004$ compared to morpholino alone). Together, these results demonstrate that PKCγ functions asymmetrically in LR development and that PKCγ is specifically required in right, but not left, ectodermal cells.

### Syndecan-2, a Putative PKCγ Target, Is Phosphorylated in Right-Side Ectoderm

If PKCγ functions asymmetrically in early LR development, endogenous targets of PKCγ should be phosphorylated in the right, but not left, ectoderm. We developed phosphospecific syndecan-2 antibodies that recognize distinct phosphorylation states of the syndecan-2 cytoplasmic domain, as well as antibodies that recognize the syndecan-2 core protein regardless of its phosphorylation state (Figure 3A).

Based on the results illustrated in Figure 1B, stage 11 appeared to be the optimal stage at which to assay for phosphorylation of PKCγ targets. To further define the window during which PKCγ regulates LR development (and theoretically syndecan-2 phosphorylation), we examined two aspects of cPKC peptide inhibitor kinetics: the rapidity of inhibitor effect and the persistence of inhibitor effect after injection. We assessed the phosphorylation state of syndecan-2 at stage 11 in embryos in which the peptide was injected at stage 9.5 (no effect on LR) or stage 10.5 (maximal effect on LR). Embryos injected at stage 10.5 had substantially decreased syndecan-2 phosphorylation within 45 min (assayed at stage 11, 14% of uninjected, Figure 3B). Thus, it is likely that the inhibitor took effect immediately. Two observations indicate that the inhibitor is only effective for approximately 1 hr after injection. Injection of peptide at stage 10 had strong effects on LR, whereas injection 1 hr earlier, at stage 9.5, had no effects on LR (Figure 1B). This suggests the inhibitor injected at stage 9.5 had

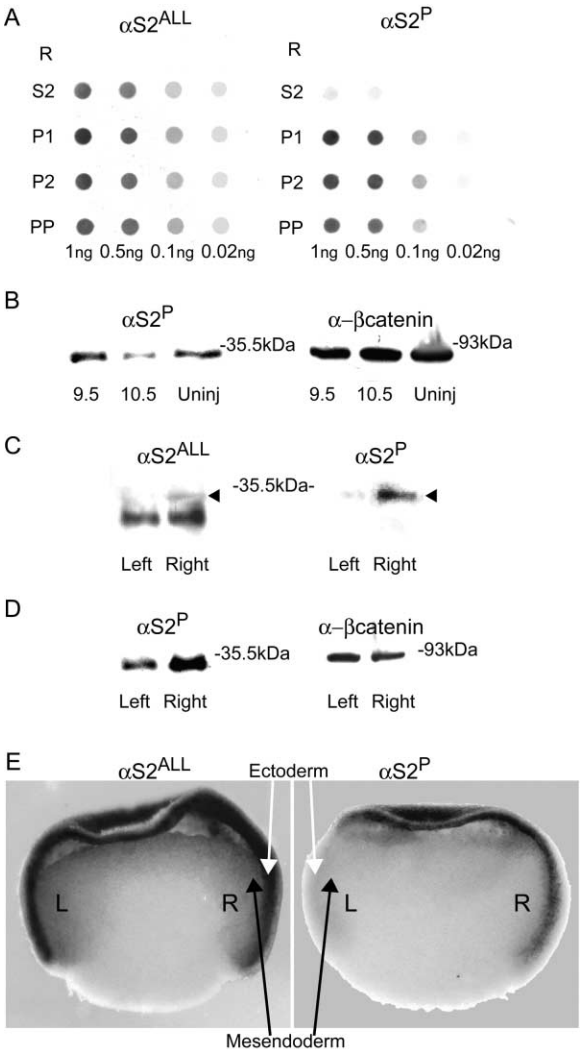


Figure 3. Endogenous Syndecan-2 Is Phosphorylated in the Right Ectoderm during Gastrulation

(A) Antibody specificity. Dot blots of chemically phosphorylated peptides used in the generation of phosphospecific antibodies. Abbreviations: R, random, nonspecific peptide; S2, unphosphorylated cGERKPS$^{150}$S$^{151}$AVY; P1, phosphorylated at S$^{150}$; P2, phosphorylated at S$^{151}$; PP, phosphorylated at S$^{150}$ and S$^{151}$. Antibody αS2$^{ALL}$ recognizes all forms of syndecan-2 peptide regardless of phosphorylation state. Antibody αS2$^{P}$ recognizes only the phosphorylated forms of syndecan-2. (B) PKC inhibitor blocks syndecan-2 phosphorylation. Embryos were injected with β-myristoylated peptide (see Figure 1) at stage 9.5, 10.5, or uninjected. At midgastrula (stage 11), extracts were immunoprecipitated with antibody 6G12, deglycosylated, and blotted with antibodies that recognize phosphorylated syndecan-2 (left). Homogenates from the same embryos were probed for β-catenin as an extract loading control (right). (C) Syndecan-2 is phosphorylated on the right side. Embryos were dissected into left and right halves at stage 11, immunoprecipitated with antibody αS2$^{ALL}$, deglycosylated, and blotted with antibodies that recognize all forms of syndecan-2 (left) or only phosphorylated syndecan-2 (right). In addition to showing the phosphorylated upper band (arrowhead), the αS2$^{ALL}$ Western blot serves as a loading control for the immunoprecipitation. (D) Extracts from embryo halves were processed as in (C) but were immunoprecipitated with the syndecan-2-specific antibody 6G12. Immunoprecipitates were probed with phosphospecific syndecan-2 antibody (left). Homogenates from the same embryo halves were probed for β-catenin as a control (right).

dissipated by stage 10. Similarly, embryos injected with inhibitor at stage 9.5 had normal levels of syndecan-2 phosphorylation (assayed at stage 11, syndecan-2 phosphorylation was 103% compared to uninjected embryos, Figure 3B). These results demonstrate that the developmental window during which cPKC function is necessary for syndecan-2 phosphorylation and LR development is brief, occurring during the first 2 hr and 45 min of gastrulation, from stages 10 to 11. Therefore, stage 11 is the optimal stage to assay for phosphorylation of syndecan-2.

Western blot analyses of stage 11 embryos dissected into left and right halves indicated that syndecan-2 core proteins were symmetrically expressed, but the cytoplasmic domain of syndecan-2 was dramatically more phosphorylated on the right (Figure 3C). When normalized to β-catenin, syndecan-2 was on average 4-fold more phosphorylated on the right than on the left (left phosphorylated syndecan-2 24% ± 9% of right from three independent experiments). Similar results were seen when previously published antibodies (Marynen et al., 1989) were used to immunoprecipitate syndecan-2 before Western blot analysis with the phosphospecific syndecan-2 antibodies (Figure 3D), further confirming the specificity of the phosphospecific syndecan-2 antibodies.

During gastrulation, syndecan-2 mRNA expression is restricted to the sensorial ectoderm, the deep layer of ectoderm that interacts with the migrating mesoderm (Teel and Yost, 1996). To confirm that syndecan-2 protein expression is similarly restricted and to examine syndecan-2 phosphorylation in situ, we performed whole-mount immunocytochemistry on stage 11 embryos. Using the antibodies that recognize syndecan-2 regardless of its phosphorylation state, syndecan-2 core protein was observed throughout the sensorial ectoderm, with a boundary of expression at both the left and right blastopore lips (Figure 3E, left). The boundary was strikingly sharp at the lip of the blastopore: noninvoluted cells that will become ectoderm expressed syndecan-2 and involuting cells that will become mesendoderm lacked syndecan-2 expression. Using the phosphospecific syndecan-2 antibodies, phosphorylated syndecan-2 was observed in the right sensorial ectoderm that was in direct contact with migrating mesoderm, but not in left sensorial ectoderm adjacent to left-side mesoderm (left and right mesoderms are marked R and L, respectively, in Figure 3E, right). These results clearly illustrate that at stage 11, left migrating mesendoderm interacts with ectoderm expressing nonphosphorylated syndecan-2, while right migrating mesendoderm interacts with ectoderm expressing phosphorylated syndecan-2. Because extensive epiboly drives animal-pole cells toward the equator before and during gastrulation

(E) Stage 11 whole-mount immunocytochemistry, using antibodies that recognize all (left) or phosphospecific (right) forms of syndecan-2. Migrating left mesoderm (L) is in contact with ectoderm that expresses nonphosphorylated syndecan-2, and right mesoderm (R) is in contact with ectoderm expressing phosphorylated syndecan-2. These illustrations are representative of over 100 embryos examined.

(Bauer et al., 1994), these differentially phosphorylated ectodermal cells are likely to be descendants of the animal cap cells targeted at the 16-cell stage with PKCγ morpholinos and at the 32-cell stage with dnPKCγ. Thus, the spatial and temporal phosphorylation of syndecan-2 in early gastrula is concomitant with the asymmetric activity of PKCγ identified by peptide inhibitor, dominant-negative, and morpholino experiments. Together, these results provide a novel vertebrate example of LR asymmetric protein phosphorylation.

### Phosphorylation of Syndecan-2 Regulates LR Development

Although unlikely, it is possible that the LR differences in phosphorylation of endogenous syndecan-2 protein do not have a role in LR development. To test the developmental functions of syndecan-2 phosphorylation, we generated phosphodeficient syndecan-2 mutants by changing the phosphoaccepting cytoplasmic serines to alanines, either as single site mutants or a double mutant in which both serines are changed to alanines. When both left and right ectoderms were targeted simultaneously with each construct, the double mutant phosphodeficient syndecan-2 randomized heart looping (S150,151A: 41% heart reversals, n = 88). In contrast, both partially phosphodeficient, single-mutant syndecan-2 constructs had an intermediate ability to disrupt normal heart looping (S150A: 35% heart reversals, n = 94; S151A: 19% heart reversals, n = 100), suggesting that the two phosphorylation sites might function in an additive and partially redundant manner.

Since the fully phosphodeficient syndecan-2 had effects that were stronger than either single serine-to-alanine mutation when injected bilaterally, we utilized it to assess whether LR development could be altered by unilateral injections of phosphodeficient syndecan-2. When phosphodeficient syndecan-2 was targeted to the right-side ectoderm, heart orientation was disrupted to a much greater extent than when it was targeted to the left side (Figure 4A). In other words, a syndecan-2 that cannot be phosphorylated acts as a dominant-negative mutant in right-side cells, but not in left-side cells. This is consistent with the results from targeting dnPKCγ or PKCγ morpholinos to the right side as well as with the observed phosphorylation of endogenous syndecan-2 only on the right side. Together, these results indicate that PKCγ activity and phosphorylation of its putative endogenous substrate, the cytoplasmic domain of syndecan-2, in right ectodermal cells are necessary for LR development.

Expression of phosphodeficient syndecan-2 had side-specific effects, suggesting that phosphorylation on the right side was obligatory for normal LR development. Therefore, we asked whether nonphosphorylation was required on the left side. Studies of several phosphoproteins have utilized the mutation of serine to glutamic acid to generate a phosphomimetic protein that structurally behaves as if the serine is constitutively phosphorylated (Thorsness and Koshland, 1987). In this case, we generated a construct in which both cytoplasmic serines of syndecan-2 were changed to glutamic acid residues. Unilateral injection of phosphomimetic syndecan-2 (S150,151E; Figure 4B) altered heart orientation, but with the opposite side specificity of the phosphodeficient syndecan-2. Heart looping was disrupted when the phosphomimetic syndecan-2 was targeted to the left ectoderm and not when it was targeted to the right ectoderm. These results support the conclusion that the phosphorylation of endogenous syndecan-2 is obligatory for normal LR development: syndecan-2 must be phosphorylated on the right and not phosphorylated on the left. Additionally, both syndecan-2 phosphorylation states, dephosphorylated in left cells and phosphorylated in right cells, have distinct side-specific regulatory roles in normal LR development.

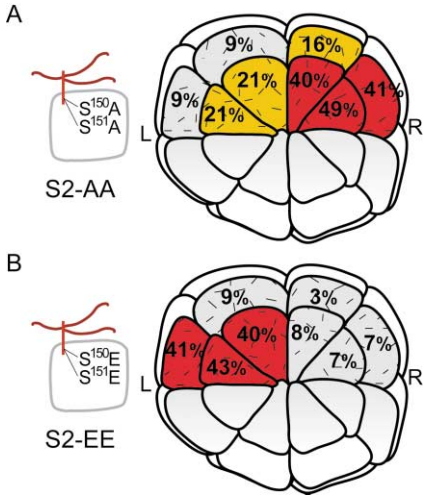


Figure 4. Both Phosphorylated Syndecan-2 on the Right and Nonphosphorylated Syndecan-2 on the Left Are Required for Normal LR Development

Percentage of reversed heart looping in embryos injected with a phosphodeficient syndecan-2 (A) or a phosphomimetic syndecan-2 (B) is shown on the right side of each panel. The left side of each panel is a diagram of the syndecan-2 constructs used in each experiment. The relative positions of the serine-to-alanine (A) or serine-to-glutamine (B) mutations are shown on the cytoplasmic domain. Wavy lines indicate the glycosaminoglycans attached to the syndecan-2 extracellular domain. See Figure 2 for an explanation of the embryo illustration. n > 55 for each cell.

Phosphodeficient and phosphomimetic syndecan-2 constructs were only targeted to the ectoderm because endogenous syndecan-2 protein is only expressed in the ectoderm (Figure 3E), and a cytoplasmically truncated dominant-negative syndecan-2 has no effect on LR development when targeted to the mesendoderm (Kramer and Yost, 2002). Nonetheless, as an additional control to demonstrate that neither construct has any activity in the mesendoderm, constructs were injected into vegetal mesendoderm precursors. Phosphodeficient syndecan-2 targeted to right mesendoderm by injecting into the right vegetal cell had no effect on LR development (4% heart reversals, n = 47). Likewise, phosphomimetic syndecan-2 targeted to left mesendoderm by injecting into the left vegetal cell had no effect on LR development (4% heart reversals, n = 49). These results support the conclusion that phosphodeficient and phosphomimetic syndecan-2 perturb LR development by specifically interrupting endogenous syndecan-2 function in the ectoderm.

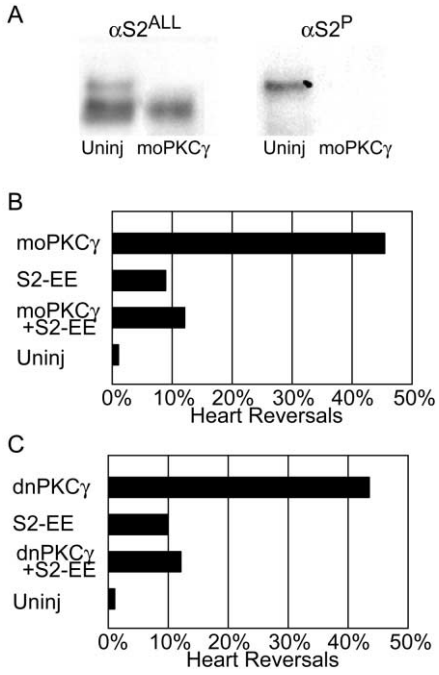


Figure 5. PKCγ Functions Upstream of Syndecan-2 in the Same LR Developmental Pathway

(A) Inhibition of PKCγ synthesis blocks phosphorylation of syndecan-2. Western blot of untreated or PKCγ-morpholino injected stage 11 embryos probed with antibodies that recognize all forms of syndecan-2 (left) or only phosphorylated (right) syndecan-2. Extracts were processed as in Figure 3. Antibody $\alpha S2^{ALL}$ serves as a loading control. (B) Epistasis analysis of PKCγ and syndecan-2. Percentage of reversed heart looping in embryos injected on the right side with morpholinos to PKCγ (moPKCγ), phosphomimetic syndecan-2 (S2-EE), or both the morpholino and the phosphomimetic syndecan-2. $n > 89$ for each injection. (C) Percentage of reversed heart looping in embryos injected with dominant-negative PKCγ (dnPKCγ), S2-EE, or both. $n > 31$ for each injection. Expression of phosphomimetic syndecan-2 rescues LR development in embryos that are deficient for PKCγ.

## PKCγ Is Upstream of Syndecan-2 Phosphorylation

PKCγ and syndecan-2 function during the same time and in the same cell lineages during LR development. Two sets of results indicate that they work in the same LR pathway. First, phosphorylation of endogenous syndecan-2 is dependent on PKCγ. Removing endogenous PKCγ by targeting xPKCγ morpholinos to the right ectoderm ablated phosphorylation of the syndecan-2 cytoplasmic domain (Figure 5A), indicating that PKCγ is upstream of syndecan-2 phosphorylation. Second, we performed a stringent test for epistasis. If PKCγ is upstream of syndecan-2 and if the sole LR role for PKCγ is to phosphorylate syndecan-2, then LR defects caused by deficiency in PKCγ function should be rescued by expression of a phosphomimetic syndecan-2 that is constitutively phosphorylated. LR development was rescued in xPKCγ morpholino-treated embryos (Figure 5B) and in dnPKCγ-treated embryos (Figure 5C) when phosphomimetic syndecan-2 was coinjected in the right ectoderm. From these results, we conclude that phosphorylated syndecan-2 functions downstream of PKCγ in the same early LR developmental pathway.

## Discussion

We have identified PKCγ as an early regulator of LR development. Syndecan-2 was previously shown to be involved in LR development (Kramer and Yost, 2002), but we did not know whether syndecan-2 functioned as a permissive cofactor or as an instructive asymmetric signal. Here, we demonstrate that syndecan-2 is phosphorylated in the right ectoderm during early gastrulation, concurrent with the period during which PKCγ activity is required in LR development. During that period, left mesendoderm migrates across ectoderm that expresses nonphosphorylated syndecan-2, while right mesendoderm migrates across ectoderm that expresses phosphorylated syndecan-2. Strikingly, both the phosphorylated syndecan-2 in the right ectoderm and nonphosphorylated syndecan-2 in the left ectoderm have roles in LR development. PKCγ phosphorylates syndecan-2, and loss of PKCγ activity can be rescued by expression of phosphomimetic syndecan-2. These results indicate that PKCγ is upstream of syndecan-2 in the same instructive LR developmental pathway that occurs prior to the formation of monocilia in *Xenopus*.

## An Early LR Developmental Timeline

From our findings, recent observations by Levin and Mercola on an early role of H+/K+-ATPase (Levin et al., 2002) and previous manipulations of the first cell cycle after fertilization (Danos and Yost, 1995; Yost, 1991), we propose a developmental timeline for early LR development in *Xenopus* (Figure 6A). This timeline illustrates that multiple asymmetric events occur before the appearance of monocilia. In *Xenopus*, the cytoplasm of the fertilized egg rotates during the first cell cycle to establish bilateral symmetry (reviewed in Yost, 1995). Normally, microtubule-dependent motors drive this rotation. Experimentally, if the rotation is driven in the absence of microtubules, normal dorsoanterior development occurs, but LR asymmetry is consistently altered (Danos and Yost, 1995; Yost, 1991). This suggests that LR asymmetry is established by events in the first cell cycle, but it is possible that this early manipulation has effects that do not ramify until late in development.

Temporally, the next event is the asymmetric distribution of a maternal RNA encoding H+/K+-ATPase in 4-cell embryos (Levin et al., 2002). Pharmacological inhibitor studies indicate that H+/K+-ATPase activity is required for normal LR development from the 4-cell stage (stage 2) to approximately (stages 6–8) the midblastula transition when the zygotic genome is activated. It is not clear whether H+/K+-ATPase is an instructive or permissive component of the early LR development, although the asymmetric RNA distribution makes it likely that it is instructive. Next, PKCγ phosphorylates syndecan-2 in animal cap ectoderm during early gastrulation (stage 10). As discussed above, both PKCγ and syndecan-2 are obligatory instructive signals in LR development. It is not known whether the PKCγ and syndecan-2 steps are dependent on asymmetric H+/K+-ATPase activity, although it is striking that all of these LR pathway components are active in the animal cap ectoderm on the ventral right side. These molecular results corroborate the suggestion from embryolog-

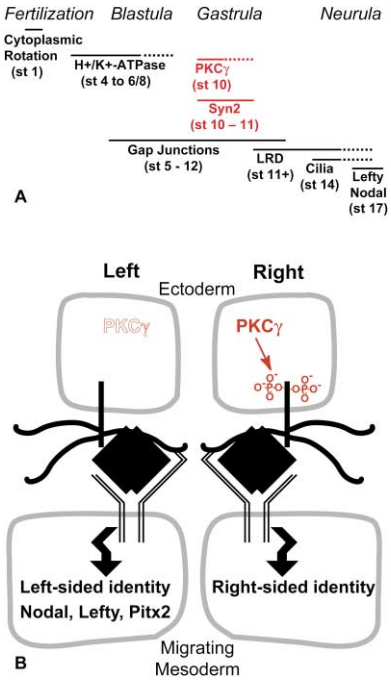


Figure 6. Syndecan-2 Is an Early Cell-Nonautonomous Transducer of LR Axis Patterning Information

(A) Timeline of *Xenopus* LR development, illustrating when each molecule has been shown to function (H + K + ATPase, gap junctions, PKCγ, and syndecan-2) or appear (asymmetric phosphorylation states of syndecan-2, *LR dynein* (*LRD*), node monocilia, and asymmetric expression of *nodal* and *lefty* in lateral plate mesoderm). See text for references. (B) A model for PKCγ-syndecan-2 function in LR development. PKCγ is either activated exclusively on the right or inhibited exclusively on the left, resulting in phosphorylation of syndecan-2 only in the right ectoderm. The LR asymmetry is transduced through syndecan-2, leading to asymmetric patterning of the mesoderm where *nodal*, *lefty*, and *pitx2* are eventually expressed only in the left mesoderm.

ical manipulations that the animal cap ectoderm has a role in LR development during gastrulation (Yost, 1992). A previously observed role for gap junctions extends from stage 5 blastula through stage 12 gastrula (Levin and Mercola, 1998). Thus, the role of gap junctions in LR development could precede or follow the roles of PKCγ and syndecan-2 and the subsequent appearance of monocilia. If all the aforementioned events occur in the same LR developmental pathway, cytoplasmic rotation could direct asymmetric H+/K+-ATPase expression, which could drive a PKCγ activator to the right side of the embryo in a gap-junction-dependent manner. Collectively, results from inhibitors, dominant-negative proteins, and antisense morpholino knockdown experiments demonstrate that multiple steps in LR axis formation occur well before the formation of monocilia.

### Is the Pathway Conserved?

It is not known whether any component of this early *Xenopus* LR pathway occurs in other vertebrates. A mouse syndecan-2 mutant has not yet been described. Treating mice embryos with broadly specific PKC inhibitors results in pleiotropic phenotypes, including neural fold and midline defects, that might mask specific roles for PKCs in LR development (Ward et al., 1998). PKCγ is expressed in the mouse oocyte and early embryo (Pauken and Capco, 2000), analogous to its temporal expression in *Xenopus*, but PKCγ mutant mice have not been reported to display LR deficiencies (Abeliovich et al., 1993a, 1993b). Other PKC isoforms have overlapping temporal and spatial expression patterns in the embryo (Pauken and Capco, 2000), opening the possibility that other PKC isoforms might be compensatory in PKCγ null mice. In contrast, the PKCγ expression pattern in *Xenopus* is spatially distinct from PKCα and PKCβ (Otte et al., 1991). Thus, it might be necessary to examine PKC double mutants in mice in order to reveal the role for PKCγ in LR development that we have been able to demonstrate here because *Xenopus* PKCγ has a spatially distinct expression pattern.

We have demonstrated that PKCγ and syndecan-2 have asymmetrically instructive roles in *Xenopus* LR development, but it is curious that the four sets of targeted injections have subtly different side specificity: PKCγ morpholino and phosphomimetic syndecan-2 disrupt normal LR development in a distinctly side-specific manner, while dnPKCγ and phosphodeficient syndecan-2 moderately (but not significantly) disrupt LR on the left while fully randomizing LR when injected on the right. In the case of PKCγ, the dominant-negative is a kinase dead protein (Freisewinkel et al., 1991) that can block endogenous PKCγ activity (Berra et al., 1993). Because similar atypical PKC constructs retain some kinase activity (Spitaler et al., 2000), the dominant-negative PKCγ might have introduced a low level of ectopic PKCγ activity to the left side of the embryo, perturbing LR. In contrast, the morpholinos provide a more straightforward elimination of PKCγ function. As for syndecan-2, we know from our earlier work that a cytoplasmically truncated syndecan-2 functions as a dominant-negative at the cell surface, presumably by interacting with endogenous syndecan-2 and inhibiting its interaction with cytoplasmic proteins that are required for normal syndecan-2 function (Kramer and Yost, 2002). Therefore, we would expect to observe a difference in syndecan-2 side specificity if these secondary interactions are limiting and required for the function of nonphosphorylated syndecan-2 on the left, but not for phosphorylated syndecan-2 on the right: phosphodeficient syndecan-2 overexpression on the left would compete for the limiting secondary interactions. Further experiments will be required to determine the exact molecular mechanism by which both the phosphorylated and nonphosphorylated syndecan-2 function in LR development.

### Proteoglycans as Inside-Out Transducers

Phosphorylation of the syndecan-2 cytoplasmic serines has been observed in cell culture (Itano et al., 1996), but the functional significance of this event in multicellular organisms is not understood. Cytoplasmic serine phosphorylation could employ several mechanisms to regulate the ability of syndecan-2 to function cell nonautonomously. Phosphorylation might mediate how migrating mesodermal cells see ectodermal syndecan-2 by controlling syndecan-2 glycosaminoglycan modification, homodimerization, or even heterodimerization with a yet unidentified molecule. Homodimerization of syndecan-2

can be regulated by phosphorylation of tyrosine residues in its cytoplasmic domain, an event critical for dendritic spine development (Ethell et al., 2001). Similarly, multimerization of syndecan-4 can be regulated by a PKC in the novel subgroup, which phosphorylates a distinct serine in syndecan-4 (Horowitz and Simons, 1998). Multimerization of syndecan-4 cell autonomously inhibits FGF-2 signal transduction (Horowitz et al., 2002). Alternatively, phosphorylation might mediate the amount of syndecan-2 at the cell surface by controlling syndecan-2 shedding or clearance. Differential shedding or clearance back into the ectoderm could change the ratio of ligands available at the cell surface. Given that both the phosphorylated and nonphosphorylated forms of syndecan-2 are obligatory for normal LR development, it is likely that the cellular mechanisms by which syndecan-2 functions are distinct on the right and left sides. Regardless of the mechanism by which syndecan-2 functions cell nonautonomously, our data demonstrate a specific role of PKCγ-dependent syndecan-2 phosphorylation in LR development.

Previously, phosphorylation of the syndecan cytoplasmic domain has been shown to be regulated downstream of receptor activation (Ethell et al., 2001; Horowitz and Simons, 1998), therefore mediating conventional outside-in signaling. In contrast, our work demonstrates that syndecan-2 signals from the inside out during LR development: ectodermal LR patterning information (differential phosphorylation of the syndecan-2 cytoplasmic domain) is transduced through syndecan-2 to pattern the mesoderm (Figure 6B). LR information drives asymmetric PKCγ activity and downstream phosphorylation of syndecan-2 in the ectoderm. Experimental alteration of syndecan-2 phosphorylation states in the ectoderm alters LR identity in migrating mesoderm that contacts the extracellular domains of syndecan-2. Thus, the nonphosphorylated form of syndecan-2 in left ectoderm transduces left-sided identity to left mesoderm, while phosphorylated syndecan-2 in right ectoderm transduces right-sided identity to right mesoderm. This work redefines the role of syndecan-2 as an instructive cofactor and demonstrates that syndecan-2 has inherent inside-out signal-transducing properties that might be applicable to a wide range of cell signaling events in development and disease.

## Experimental Procedures

### Embryo Treatments and Injections

For chelerythrine chloride treatment, embryos were placed into 10 μM chelerythrine chloride in 1/3 MMR 15 min after fertilization and incubated in the solution at room temperature until stage 15 of development. The embryos were subsequently washed with 1/3 MMR and maintained in 1/3 MMR for 4 additional days until they were scored for the direction of heart looping. Cell-permeable myristoylated peptides (BioMol) that block conventional (β C2-4), novel (ε V1-2), or atypical (ζ) PKCs were injected (25–50 μM) into the blastocoel of early gastrula-stage *Xenopus* embryos. For cell-lineage injections, 8-cell stage embryos were selected that displayed a regular cleavage pattern where one of the two meridional cleavages creates a bilaterally symmetrical pigmentation pattern. Embryos were further selected at the 32-cell stage in which blastomeres were arranged as four distinctive tiers of eight cells each. Both ventral animal-pole cells (or as specified in the results) were each injected with 0.5–1 ng mRNA of the indicated construct. In all cases, the direction of heart looping was scored 5 days postfertilization. p values were generated by $\chi^2$ analyses and refer to the null hypothesis that experimental and rescue embryos are equivalent. Embryo culture, left-right analysis, RNA synthesis, and in situ hybridization followed previously described protocols (Kramer and Yost, 2002).

### Xenopus PKCγ Cloning

RNA was isolated from late blastula stage *Xenopus* embryos by TriReagent extraction (Molecular Research Center, Inc.). Reverse transcription of total RNA was performed with Superscript II (Invitrogen), and PCR amplifications of a 670 bp fragment were carried out using Platinum Taq (Invitrogen) with degenerate primers (5′-CCACAGACAGATGATCCAAGAAATAARCAYAARTT-3′ and 5′-TTC GTACAGTTCCAGTGGGTAATTRCANGCYTC-3′). All amplified fragments were cloned into pCRII using the Topo cloning kit (Invitrogen), subsequently sequenced, and the resulting sequence was used to design primers for 5′ RACE. Capped, full-length 5′ clones were isolated using GeneRacer (Invitrogen) as described by the manufacturer, except reverse transcription was done using the PKCγ primer: 5′-GCGTCGTCAGATACTGGGACATTGTA-3′. The first round of PCR was done using GeneRacer 5′ primer with 5′-ACCAGCCATCCA CAGCATTCTTCAT-3′, and a second round was done using GeneRacer 5′ Nested primer with 5′-CAGCTCCTGGACATTCAAAG-3′. An equal number of full and short PKCγ clones were obtained from this, as well as a completely independent round of 5′ RACE cloning. Additional details and sequence data are provided in the supplemental data (see Supplemental Figure S1). Morpholinos were synthesized by Gene Tools, LLC.

### Phospho-Antibody Production

Four peptides corresponding to the cytoplasmic domain of syndecan-2 (cGERKPSSAVY with the underlined serines either unphosphorylated or chemically phosphorylated at the first serine, second serine, or both serines) were synthesized at the University of Utah DNA/Peptide Facility. Peptides were subsequently conjugated to KLH (mcKLH-Pierce) and used to immunize rabbits at Harlan Bioproducts for Science, Inc. Specificity and titer were determined by dot blot. Antibodies were affinity purified using peptides conjugated to UltraLink Iodoacetyl (Pierce) and eluted using either Immunopure IgG Elution Buffer (Pierce) or 3.5 M $MgCl_2$. After dialysis and concentration (CentriPlus, Millipore), antibodies were further characterized by dot blot, immunoprecipitation, and Western blotting, using techniques as previously described (Kramer and Yost, 2002) except glycosaminoglycan side chains were removed after immunoprecipitation as described by Ethell et al. (2001), and Western blots were blocked with 1%BSA / 1% polyvinylpyrrolidone in TBST. For collecting stage 11 left and right embryo halves, 4-cell embryos were first selected using the same approach for RNA injection (see above), but one-half of the embryo was injected with Texas Red dextran (Molecular Probes). At stage 11, 20 embryos were bisected along the fluorescent border and processed for immunoprecipitation and Western blotting. No bands appear on the gel other than those we show (see Supplemental Figure S2 online at http://www.cell.com/cgi/content/full/111/7/981/DC1). Densitometry was determined using a Storm Phosphorimager. The PKCγ antibody was against the C-terminal region of PKCγ and was obtained from Oxford Biomedical Research, while the β-catenin antibody was from Zymed.

### Whole-Mount Immunocytochemistry

Stage 10 albino embryos were marked with Nile blue (Sigma) at the dorsal lip, collected at stage 11, and fixed in 4% paraformaldehyde with 0.1 M MOPS (pH 7.4), 2 mM EGTA, and 1 mM $MgSO_4$ at room temperature for 2 hr. The vitelline membranes were removed 10 min into the fixation process. After fixation, the embryos were cut into dorsal and ventral halves using the dye mark as a dorsal marker. The embryos were then rinsed several times in PBST, dehydrated through an ethanol series, and stored in glass vials in methanol overnight at −20°C. For the experiment, embryos were rehydrated through a methanol series to PBST and subsequently washed (PBST + 1% DMSO + 1% BSA). The embryos were transferred to a 24-well dish and blocked at room temperature for 1 hr in 10% filtered, heat-inactivated sheep serum with 1% DMSO and 1% BSA in PBST. Primary syndecan-2 antibodies were diluted 1:1000 in fresh blocking buffer and incubated overnight at 4°C. Embryos were

washed and reblocked in fresh blocking buffer for 30 min. Alkaline phosphatase (AP)-conjugated anti-rabbit secondary antibody (Jackson Laboratories) was diluted 1:2000 in fresh blocking buffer and applied overnight at 4°C. Embryos were washed in wash buffer and then in AP reaction buffer (0.1 M Tris [pH 9.5], 50 mM $MgCl_2$, 0.1 M NaCl, and 0.1% Tween-20). The AP reaction was developed with NBT (4.5 μl/ml) and BCIP (3.5 μl/ml) reagents (Roche). The embryos were then washed in PBST and photographed. All washes and incubations were done at room temperature with slight shaking unless otherwise noted.

## Acknowledgments

We thank Bill Bradford, Brandon Burbach, Maureen Condic, Jeff Essner, and David Virshup for helpful suggestions; Mark Mercola for discussions and sharing unpublished observations; and Guido David, Randall Moon, and Ajit Verma for reagents. K.L.K. was supported by a NRSA from NIH/NIHLB. Core facilities are supported by NCI CCSG. This work was supported by grants to H.J.Y. from an NIH/NIHLB SCOR program and the Huntsman Cancer Foundation.

Received: August 21, 2002
Revised: November 14, 2002

## References

Abeliovich, A., Chen, C., Goda, Y., Silva, A.J., Stevens, C.F., and Tonegawa, S. (1993a). Modified hippocampal long-term potentiation in PKC gamma-mutant mice. Cell *75*, 1253–1262.

Abeliovich, A., Paylor, R., Chen, C., Kim, J.J., Wehner, J.M., and Tonegawa, S. (1993b). PKC gamma mutant mice exhibit mild deficits in spatial and contextual learning. Cell *75*, 1263–1271.

Bamford, R.N., Roessler, E., Burdine, R.D., Saplakoglu, U., dela Cruz, J., Splitt, M., Towbin, J., Bowers, P., Marino, B., Schier, A.F., et al. (2000). Loss-of-function mutations in the EGF-CFC gene CFC1 are associated with human left-right laterality defects. Nat. Genet. *26*, 365–369.

Bauer, D.V., Hyang, S., and Moody, S.A. (1994). The cleavage stage origin of Spemann's Organizer: analysis of the movements of blastomere clones before and during gastrulation in *Xenopus*. Development *120* 1179–1189.

Berra, E., Diaz-Meco, M.T., Dominguez, I., Municio, M.M., Sanz, L., Lozano, J., Chapkin, R.S., and Moscat, J. (1993). Protein kinase C zeta isoform is critical for mitogenic signal transduction. Cell *74*, 555–563.

Capdevila, J., Vogan, K.J., Tabin, C.J., and Izpisua Belmonte, J.C. (2000). Mechanisms of left-right determination in vertebrates. Cell *101*, 9–21.

Danos, M.C., and Yost, H.J. (1995). Linkage of cardiac left-right asymmetry and dorsal-anterior development in Xenopus. Development *121*, 1467–1474.

Essner, J.J., Vogan, K.J., Wagner, M.K., Tabin, C.J., Yost, H.J., and Brueckner, M. (2002). Left right development: conserved function for embryonic nodal cilia. Nature *418*, 37–38.

Ethell, I.M., Irie, F., Kalo, M.S., Couchman, J.R., Pasquale, E.B., and Yamaguchi, Y. (2001). Ephb/syndecan-2 signaling in dendritic spine morphogenesis. Neuron *31*, 1001–1013.

Freisewinkel, I., Riethmacher, D., and Stabel, S. (1991). Downregulation of protein kinase C-gamma is independent of a functional kinase domain. FEBS Lett. *280*, 262–266.

Gaio, U., Schweickert, A., Fischer, A., Garratt, A.N., Muller, T., Ozcelik, C., Lankes, W., Strehle, M., Britsch, S., Blum, M., and Birchmeier, C. (1999). A role of the cryptic gene in the correct establishment of the left-right axis. Curr. Biol. *9*, 1339–1342.

Gritsman, K., Zhang, J., Cheng, S., Heckscher, E., Talbot, W.S., and Schier, A.F. (1999). The EGF-CFC protein one-eyed pinhead is essential for nodal signaling. Cell *97*, 121–132.

Hamada, H., Meno, C., Watanabe, D., and Saijoh, Y. (2002). Establishment of vertebrate left-right asymmetry. Nat. Rev. Genet. *3*, 103–113.

Horowitz, A., and Simons, M. (1998). Regulation of syndecan-4 phosphorylation in vivo. J. Biol. Chem. *273*, 10914–10918.

Horowitz, A., Tkachenko, E., and Simons, M. (2002). Fibroblast growth factor-specific modulation of cellular response by syndecan-4. J. Cell Biol. *157*, 715–725.

Hyatt, B.A., Lohr, J.L., and Yost, H.J. (1996). Initiation of vertebrate left-right axis formation by maternal Vg1. Nature *384*, 62–65.

Itano, N., Oguri, K., Nagayasu, Y., Kusano, Y., Nakanishi, H., David, G., and Okayama, M. (1996). Phosphorylation of a membrane-intercalated proteoglycan, syndecan-2, expressed in a stroma-inducing clone from a mouse Lewis lung carcinoma. Biochem. J. *315*, 925–930.

Kramer, K.L., and Yost, H.J. (2002). Ectodermal syndecan-2 mediates left-right axis formation in migrating mesoderm as a cell-nonautonomous vg1 cofactor. Dev. Cell *2*, 115–124.

Levin, M., and Mercola, M. (1998). Gap junctions are involved in the early generation of left-right asymmetry. Dev. Biol. *203*, 90–105.

Levin, M., Thorlin, T., Robinson, K., Nogi, T., and Mercola, M. (2002). Asymmetries in H+/K+-ATPase and cell membrane potentials comprise a very early step in left-right patterning. Cell *111*, 77–89.

Marynen, P., Zhang, J., Cassiman, J.J., Van den Berghe, H., and David, G. (1989). Partial primary structure of the 48- and 90-kilodalton core proteins of cell surface-associated heparan sulfate proteoglycans of lung fibroblasts. J. Biol. Chem. *264*, 7017–7024.

Meno, C., Ito, Y., Saijoh, Y., Matsuda, Y., Tashiro, K., Kuhara, S., and Hamada, H. (1997). Two closely-related left-right asymmetrically expressed genes, lefty-1 and lefty-2: their distinct expression domains, chromosomal linkage and direct neuralizing activity in Xenopus embryos. Genes Cells *2*, 513–524.

Nonaka, S., Tanaka, Y., Okada, Y., Takeda, S., Harada, A., Kanai, Y., Kido, M., and Hirokawa, N. (1998). Randomization of left-right asymmetry due to loss of nodal cilia generating leftward flow of extraembryonic fluid in mice lacking KIF3B motor protein. Cell *95*, 829–837.

Nonaka, S., Shiratori, H., Saijoh, Y., and Hamada, H. (2002). Determination of left right patterning of the mouse embryo by artificial nodal flow. Nature *418*, 96–99.

Oh, E.S., Couchman, J.R., and Woods, A. (1997). Serine phosphorylation of syndecan-2 proteoglycan cytoplasmic domain. Arch. Biochem. Biophys. *344*, 67–74.

Okada, Y., Nonaka, S., Tanaka, Y., Saijoh, Y., Hamada, H., and Hirokawa, N. (1999). Abnormal nodal flow precedes situs inversus in iv and inv mice. Mol. Cell *4*, 459–468.

Otte, A.P., Kramer, I.M., and Durston, A.J. (1991). Protein kinase C and regulation of the local competence of Xenopus ectoderm. Science *251*, 570–573.

Pauken, C.M., and Capco, D.G. (2000). The expression and stage-specific localization of protein kinase C isotypes during mouse preimplantation development. Dev. Biol. *223*, 411–421.

Prasthofer, T., Ek, B., Ekman, P., Owens, R., Hook, M., and Johansson, S. (1995). Protein kinase C phosphorylates two of the four known syndecan cytoplasmic domains in vitro. Biochem. Mol. Biol. Int. *36*, 793–802.

Ron, D., Luo, J., and Mochly-Rosen, D. (1995). C2 region-derived peptides inhibit translocation and function of beta protein kinase C in vivo. J. Biol. Chem. *270*, 24180–24187.

Ryan, A.K., Blumberg, B., Rodriguez-Esteban, C., Yonei-Tamura, S., Tamura, K., Tsukui, T., de la Pena, J., Sabbagh, W., Greenwald, J., Choe, S., et al. (1998). Pitx2 determines left-right asymmetry of internal organs in vertebrates. Nature *394*, 545–551.

Shen, M.M., and Schier, A.F. (2000). The EGF-CFC gene family in vertebrate development. Trends Genet. *16*, 303–309.

Spitaler, M., Villunger, A., Grunicke, H., and Uberall, F. (2000). Unique structural and functional properties of the ATP-binding domain of atypical protein kinase C-iota. J. Biol. Chem. *275*, 33289–33296.

Teel, A.L., and Yost, H.J. (1996). Embryonic expression patterns of Xenopus syndecans. Mech. Dev. *59*, 115–127.

Thorsness, P.E., and Koshland, D.E., Jr. (1987). Inactivation of isoci-

trate dehydrogenase by phosphorylation is mediated by the negative charge of the phosphate. J. Biol. Chem. *262*, 10422–10425.

Ward, K.W., Rogers, E.H., and Hunter, E.S., 3rd. (1998). Dysmorphogenic effects of a specific protein kinase C inhibitor during neurulation. Reprod. Toxicol. *12*, 525–534.

Wright, C.V. (2001). Mechanisms of left-right asymmetry: what's right and what's left? Dev. Cell *1*, 179–186.

Yan, Y.T., Gritsman, K., Ding, J., Burdine, R.D., Corrales, J.D., Price, S.M., Talbot, W.S., Schier, A.F., and Shen, M.M. (1999). Conserved requirement for EGF-CFC genes in vertebrate left-right axis formation. Genes Dev. *13*, 2527–2537.

Yost, H.J. (1991). Development of the left-right axis in amphibians. Ciba Found. Symp. *162*, 165–176.

Yost, H.J. (1992). Regulation of vertebrate left-right asymmetries by extracellular matrix. Nature *357*, 158–161.

Yost, H.J. (1995). Vertebrate left-right development. Cell *82*, 689–692.